
Title: Friedman and n-reaction order methods applied to pine needles and polyurethane thermal decompositions

Authors: R. Font, M.A. Garrido

PII: S0040-6031(18)30002-9
DOI: https://doi.org/10.1016/j.tca.2018.01.002
Reference: TCA 77911

To appear in: *Thermochimica Acta*

Received date: 17-10-2017
Revised date: 29-12-2017
Accepted date: 1-1-2018

Please cite this article as: R.Font, M.A.Garrido, Friedman and n-reaction order methods applied to pine needles and polyurethane thermal decompositions, Thermochimica Acta https://doi.org/10.1016/j.tca.2018.01.002

# Friedman and n-reaction order methods applied to pine needles and polyurethane thermal decompositions

*R. Font*, M. A. Garrido*

Department of Chemical Engineering, University of Alicante, P.O. Box 99, E-03080 Alicante (Spain)

*Email: rafael.font@ua.es

**Highlights:** Friedman method can be applied to different runs

- A temperature reference is useful to correlate the pre-exponential factor
- Different variations of parameters are correct to simulate the data
- The fitting models must only be considered valid to simulate the data

**Abstract**

The Friedman method is applied to two processes: flexible polyurethane foam (PU) pyrolysis and pine needle combustion, considering two types of runs: dynamic and dynamic + isothermal. In both cases, the TG and DTG runs are taken into account. For both materials, the Friedman method is applied twice: one considering only the dynamic runs and the other considering all runs, dynamic and dynamic + isothermal runs. Different expressions for fitting the variation of the apparent activation energy and the pre-exponential function have been obtained and used to simulate the experimental results.

The simulated results are compared with the experimental ones and with those simulated with the n-reaction order models. From the discussion carried out, it has been deduced that the Friedman method is valid when taking into account all the experimental data obtained in different operating conditions and after testing that the simulated results are close to the experimental ones.

**Keywords:** Friedman method, n-reaction order kinetic methods, pyrolysis, combustion

## 1. Introduction

Thermogravimetric analysis (TGA) is an analytical technique used for measuring the weight change of a material during heating under controlled conditions, such as constant temperature (isothermal runs), constant heating rate (non-isothermal or dynamic runs) or combining both (dynamic + isothermal runs). The kinetics of mass loss of materials during their thermal decomposition is required for the characterization and system design [1].

Different kinetic models have been presented in the literature which can be classified into two main groups: fitting-model or free-model. The main difference between both types of models is that while the fitting-model is based on the assumption that the decomposition followed a particular reaction model, the free-model allows the determination of the activation energy without proposing any specific mechanism or reaction model for the transformation [2].

Between the fitting-models, the n-reaction order model, considering one or many fractions, has been extensively used, although others models such as the Distributed Apparent Energy Model (DAEM) have also been used. A comparison between the n-reaction order and the DAEM model and other models can be found in the literature [3]. It was shown that when the distribution of the apparent activation energy obtained in the DAEM model is small, the same results can probably be satisfactorily correlated by the n-reaction order model. In the n-reaction order model, for each fraction considered the maximum fraction volatilized must be considered, in addition to the three characteristic kinetic parameters: pre-exponential factor, apparent activation energy and reaction order

[3]. This model presents the advantage of being able to reproduce the experimental data from different operating conditions, using a single set of kinetic parameters, which remains constant during the decomposition process. It can be applied to small fractions, such as humidity, whose evolved volatiles can be different for some samples. The same model with n-reaction order kinetics can be applied in different atmospheres, but considering the partial pressure of the reactant gas, e.g. oxygen, in combustion reactions.

In general, the rate of many thermally stimulated processes can be parameterized in terms of temperature, T, and conversion degree, α ($0 \leq \alpha \leq 1$) [4, 5] as follows:

$$\frac{d\alpha}{dt} = f(\alpha)k(T) \quad (1)$$

where f(α) is the reaction model which depends on the reaction mechanism, k(T) is the temperature-dependent rate constant [6]. For decomposition processes of a solid/liquid inside a crucible of a TG apparatus or a vessel where the total mass is monitored vs. time, the conversion degree can be defined by the following eq. (2):

$$\alpha = \frac{m_0 - m_t}{m_0 - m_f} \quad (2)$$

where $m_0$, $m_f$ and $m_t$ are the sample masses at the beginning, at the end and at a given time t.

For chemical transformations, the k(T) is usually expressed with the Arrhenius dependence:

$$k(T) = ke^{-E/RT} \quad (3)$$

where $k_0$ is the pre-exponential factor, E is the activation energy and R is the gas constant. Including the Arrhenius expression in the eq. (1), the general expression for a single step kinetic equation is obtained [7]:

$$\frac{d\alpha}{dt} = kf(\alpha)e^{-E/RT} \quad (4)$$

For decomposition studies performed at a constant heating rate (dynamic runs), a great number of methods have been developed for deriving the activation energy [8]. All the methods for obtaining the activation energy require the determination of the T at a fixed conversion degree for 3–5 runs at different heating rates [4, 9].

Although there are many iso-conversional methods, the analysis presented in this paper is done only with the Friedman method [10]. The method is based on the equation obtaining by taking the logarithm in eq. (4), and substituting the symbol $k_o$ by the parameter A, assuming that the term Af(α) is a function of α, as shown as:

$$ln\left(\frac{d\alpha}{dt}\right)_{\alpha,i} = ln\big(Af(\alpha)\big) - \frac{E_\alpha}{RT_{\alpha,i}} \qquad (5)$$

Hence for runs performed at different heating rates, $\beta_i$, Af(α) will be constant at a fixed conversion degree, α [11]. By measuring the temperature, T and the reaction rate, dα/dt, at the fixed conversion degree, α, for all experiments performed at different heating rates, the activation energy can be calculated from the slope of the representation of $\ln(d\alpha/dt)_{\alpha,i}$ vs $1/T_{\alpha,i}$ whereas from the intercept $\ln(Af(\alpha)k_0)$ is obtained [12-22]. Whilst this differential method does not employ any mathematical approximation, as in the case of other integral methods, it can be considered as more accurate than the integral ones. However, these methods present the handicap of being really sensitive to the determination of baseline and calibration of the thermal analysis equipment introducing significant inaccuracy in the reaction rate dα/dt [4, 8]. On the other hand, the Friedman model can also be applied to any type of run: dynamic, isothermal, dynamic + isothermal, ramps, etc., with the only consideration that the values of $\ln(d\alpha/dt)_{\alpha,i}$ must be correctly determined. In this paper, the Friedman model is applied to dynamic runs only and to dynamic and dynamic+isothermal runs and the kinetic parameters are compared between themselves and with those obtained by the n-reaction order model.

## 2. Experimental

### *2.1 Raw materials*

Table 1 shows the moisture, elemental analysis and net calorific value for two materials: flexible PolyUrethane foam (PU) and pine needles. Moisture was determined as the weight loss after 12 h at 105ºC whereas for the ash content the samples were calcinated at 850ºC for 8 h. The CHNS analysis was carried out in a Perkin Elmer 2400 (Perkin Elmer, UK) and the calorific values were obtained employing an AC-350 calorimetric bomb from Leco Corporation.

Table 1

### *2.2 Thermobalance experiments*

The experimental data employed in this work are the same as those corresponding to the pyrolysis runs presented in previous articles from the kinetic study of PU [23] and pine needles [24]. A summary of the experimental conditions can be found in Table 2.

Table 2

Pyrolysis runs of PU were carried out in a Perkin Elmer thermobalance model TGA/SDTA-6000 with a vertical furnace and a single beam vertical balance was employed. On the other hand, the combustion runs of pine needles were performed in a TAG/SDT 851e/LF/1600 Mettler Toledo thermobalance with a horizontal furnace and a parallel-guided balance

## 3 Results and discussion

### *3.1. Flexible Polyurethane foam (PU) pyrolysis process kinetic study*

#### *3.1.1 PU. n-reaction order model*

Garrido and Font [23] proposed a model consisting of two consecutive reactions for the pyrolysis of PU (Scheme 1), with n-reaction order kinetics for each reaction, with the first decomposition step at about 550 K and the second at about 640 K. It was tested that the first decomposition step corresponded to the break of the urethane bond to obtain mainly isocyanates and in the second, the decomposition of ether polyols took place.

$$PU \xrightarrow{1} (1 - v_{1\infty})products_1 + v_{1\infty}volatiles_1$$

$$(1 - v_{1\infty})products_1 \xrightarrow{2} (1 - v_{2\infty})residue + v_{2\infty}volatiles_2$$

Scheme 1. Reactions considered for the pyrolytic model of FPUF.

Table 3 shows the kinetic parameters obtained from the fitting to the n-reaction order model, the pre-exponential factor $k_{io}$ , the apparent activation energy $E_i$ and the reaction order $n_i$ for each decomposition obtaining also the maximum mass fraction of volatiles evolved $V_{i\infty}$.

Table 3

Figures 1a and 1b show the results obtained for two runs: the dynamic at 10 K/min and the dynamic + isothermal run (10 K/min to 633 K and then maintaining the temperature constant). In both Figures, the TG and DTG plots are presented for the experimental results, the simulated results by the n-reaction order model and by the Friedman method, considered and discussed later. In the three cases, the coincidence is total and the same occurs for the remaining runs.

Figure 1

### *3.1.2 PU. Friedman method considering only the dynamic runs*

The values of ln(dα/dt) were calculated for each α inside the interval [ 0.05 – 0.95] with a 0.05 step for the three dynamic runs performed, in accordance with eq. (5). For each α, the linear regressions of ln(dα/dt) vs. 1/T data were obtained and the corresponding slopes (-E/R) and intercepts on the Y-axis (lnAf(α)) were obtained. Table 4 shows the

correlation coefficients and the values of activation energy (deduced form the slopes) The values of (ln(Af(α))) - E/RTm, which is equivalent to ln(Af(α)exp(-E/RTm)), for each α, taking the corresponding values of ln(Af(α)) and E, have been obtained considering a reference temperature inside the temperature interval where the decomposition rates are high. In this case, the reference temperature was 600 K. In this way, the fitting of the kinetic parameters was better than when this factor was not included, reducing the compensation effect between the two parameters E and Af(α). Note that Af(α)exp(-E/RTm) represents the value of the kinetic constant calculated for each α but for the same temperature Tm.

Table 4

Most of the $r^2$ values shown in Table 4 are higher than 0.94, but there also some low values. Figures 2a and 2b show the variations of the apparent activation energy in two ranges in order to obtain acceptable correlation coefficients. In both Figures, the values deduced from Table 4 and those obtained by the fittings carried out are presented.

Figure 2

Figure 3 shows the variation of ln(Af(α)exp(-E/RTm)) vs. α, considering a value of 600K for the temperature Tm, taking the value of E deduced for each α. The values deduced from Table 4 and those calculated from the fittings can be observed.

Figure 3

From the fittings equation previously deduced, the parameter E/R and Af(α) can be calculated for any values of α inside the interval considered using the fitting polynomic equations deduced. Many significant figures have been considered to avoid mathematical errors. It is assumed that the equations can be valid from all the intervals of α, which is from 0 to 1. For each value of α, the value of Af(α) must be calculated as

follows: 1) Calculate ln(Af(α)exp(-E/RTm)) from the corresponding polynomic equation shown in the upper part of Figure 3, 2) Calculate Af(α)exp(-E/RTm) from the previous value, 3) Calculate E by the corresponding polynomic equation shown in the upper part of Figure 2, 4) Calculate exp(-E/RTm) from the previous value of E and the temperature reference (600 K), and 5) Divide the value of Af(α)exp(-E/RTm) by the value of exp(-E/RTm) to obtain the value of Af(α).

Integrating eq. 4, by the Euler method with very small intervals of time and considering the experimental temperature, the variation of α is obtained. The calculated values for both TG and DTG are plotted in Figure 1a for a run, observing a coincidence with the experimental results and with the n-reaction order model.

Figure 1b also shows the experimental values, those calculated with the n-order reaction and the Friedman method for one of the three dynamic + isothermal runs, whose data were used for the fitting of the n-order model but not for the Friedman method. It is remarkable that the fitting parameters obtained by the Friedman method considering only dynamic runs are also valid for simulating the dynamic+isothermal runs.

Considering the values of the apparent activation energy by the Friedman method, it can be observed that most values are around 100-120 kJ/mol, which is different to apparent activation energies of the two stages considered by the n-order model, 142 and 217 kJ/mol, obtained from the fitting of dynamic and dynamic + isothermal runs.

### 3.2.2 PU. Friedman method considering the dynamic runs and the dynamic and dynamic + isothermal runs.

The same analysis, using the Friedman method, has been carried out but this time considering dynamic and dynamic + isothermal runs. Table 5 shows the correlation coefficients and the values deduced from the fitting parameters.

Table 5

Figure 4 shows the variation of the apparent activation energy and the fitting equations in two intervals, for better fitting.

Figure 4

The variation of $\ln(Af(\alpha)\exp(-E/RTm))$ vs. $\alpha$, in this case, considering also the value of 600 K for the temperature that can be observed in Figure 5. The values deduced from Table 4 and those calculated from the fittings can be observed.

Figure 5

Figure 6 shows the calculated variations by the Friedman method, considering the dynamic and the dynamic + isothermal runs, together with the experimental results and those calculated by the n-order reaction model. The coincidence of results is also nearly total. In this case, the apparent activation energies from the Friedman model are between 135 and 179 kJ/mol from $\alpha$ 0.05 to 0.4 and between 187 and 213 kJ/mol from $\alpha$ 0.45 to 0.95. These intervals are close to the two apparent activation energies 142 (first decomposition) and 217 kJ/mol (second decomposition) of the n-reaction order model in this case.

Nevertheless, it can be observed that the two sets of variation of E and $Af(\alpha)$ reproduce satisfactorily both dynamic and dynamic + isothermal runs. Probably, the great interrelation between the reaction order and the pre-exponential factor leads to many acceptable solutions. Therefore, in both cases, the deduced expressions are only valid for fitting the experimental results, without a clear chemical-physical meaning.

Figure 6

### *3.2 Pine needles combustion process kinetic study*

The same procedure previously described is carried out with pine needles.

#### 3.2.1 Pine needles. n-reaction order model

Font et al. [24] studied the kinetics of pyrolysis and combustion of pine needles and cones. Considering the lumping model and the n-reaction order kinetics, the kinetic parameters were obtained from 17 runs (dynamic and dynamic + isothermal) from three atmospheres: nitrogen, nitrogen: oxygen 4:1 and 9:1 ratios. Table 6 shows the complex scheme of reactions proposed and the kinetic model for each reaction. Table 7 shows the values of the kinetic parameters and some considerations to analyze the coherence of the model.

Tables 6 and 7

Figures 7a and 7b shows the comparison of experimental and calculated values of two runs, the deviations are also small in the remaining tests. The results obtained by the Friedman method are also presented.

Figure 7

#### *3.2.2. Pine Needles. Friedman method considering only the dynamic runs*

The Friedman method is applied within the interval [0.07 – 0.95] with a 0.05 step for the three dynamic runs performed. For each $\alpha$, the linear regressions of $\ln(d\alpha/dt)$ vs. $1/T$ data from three experiments at different heating rates were obtained and the values deduced from fitting parameters are shown in Table 8.

Table 8

From Table 8 and following a similar procedure to that previously explained, Figures 8 (with two intervals) and Figure 9 show the variations and fitting correlations of E and ln(Af(α)exp(-E/RTm)).

Figures 8 and 9

With the equations proposed in Figures 10 and 11, the experimental data have been simulated following the method explained previously by the integration of eq. (5).

Figure 7a shows the simulated data for a dynamic run, observing a coincidence in the TG variation and small deviations in the DTG plot. Similar results are obtained for the other two dynamic runs.

Figure 7b also shows the simulated data for a dynamic + isothermal run, observing a deviation with respect to the experimental results and the same occurs with the other four dynamic + isothermal runs. Therefore, in this case, the data obtained by the Friedman method from the dynamic runs only are not valid to simulate the dynamic + isothermal runs. In the following section, the analysis is carried out considering all runs.

### *3.2.3. Pine Needles. Friedman method considering both the dynamic runs and the dynamic + isothermal runs*

Table 9 shows the results when applying the Friedman method to dynamic and dynamic + isothermal runs. From this Table, the fitting equations shown in Figures 10 and 11 are shown. The simulated values are shown in Figure 12.

Table 9 and Figures 10 to 12

From Figure 12, it can be deduced that the fitting equations of E and Af(α) obtained considering all runs are useful to satisfactorily correlate the two runs shown. The same also occurs with the other two dynamic runs and with the other four dynamic + isothermal runs.

A critical study of the isoconversional methods was carried out by Criado et al. [25]. They concluded that when a variation of the activation energy vs. conversion is assumed, the Friedman provides accurate values of activation energy, whereas a scheme of reactions is proposed, then the activation energy calculated depend on the heating rate. From the analysis carried out in this paper, when there are correlation coefficients far from 1, it can be deduced that the variation of the kinetic parameters only on the conversion is not correct, but in spite of this fact, acceptable correlations can be obtained by the Friedman method because there are mathematical compensations.

On the other hand, it must be emphasized that experimental data obtained in different operation conditions must be analyzed by the Friedman method in order to obtain an acceptable correlation valid for cases.

## 4. Conclusions

The Friedman method is valid to obtain satisfactory fitting equations to simulate the experimental results. It has been tested that the fitting of ln(Af(α)exp(-E/RTm)) using a reference temperature vs. the conversion degree α is adequate for obtaining good results.

From the experimental data of flexible polyurethane foam pyrolysis, two different sets of fitting equations have been deduced by the Friedman method: one set considering only the dynamic runs and the other set from dynamic and dynamic+ isothermal runs.

Both sets simulate the experimental results of all runs correctly. Furthermore, the TG and DTG curves obtained from the Friedman method are close to those simulated by the n-reaction order model considering two consecutive reactions. The differences between the two sets of equations corresponding to the variations of the apparent activation energy E and Af(α) are considerable, indicating that these equations must be considered valid only for fitting the experimental data.

Nevertheless, applying the Friedman method to the pine needle combustion, only when all data are considered (dynamic and dynamic + isothermal runs) are the fitting equations valid to correctly simulate all the results. When only the dynamic runs are taken into account, the fitting equations obtained are valid to simulate the dynamic runs but not the dynamic + isothermal runs.

From the previous results, it is proposed that the Friedman method must be applied to all the runs obtained in different experimental conditions and the simulated results must be obtained to observe if the fitting equations are valid or not.

It can also be concluded that the fitting equations must be considered valid only to simulate the results, because there can be more than one set of E and Af(α) fitting equations that satisfactorily reproduce the experimental results, so the possible chemical-physical significance must be deduced considering other analyses.

***Acknowledgment Support***: Research Project CTQ2016-76608-R (Spanish Ministry Economia/Competividad Spain), and PROMETEOII/2014/00 (Generalitat Valenciana, Spain

**References**

[1] M. Fernandez-Lopez, G.J. Pedrosa-Castro, J.L. Valverde, L. Sanchez-Silva, Kinetic analysis of manure pyrolysis and combustion processes, Waste Management, 58 (2016) 230-240.
[2] J. Farjas, P. Roura, Isoconversional analysis of solid state transformations, Journal of Thermal Analysis and Calorimetry, 105 (2011) 757-766.
[3] R. Font, Potential kinetic model for thermal decomposition of complex organic compounds: Significance of parameters and engineering application, Thermochimica Acta, 591 (2014) 81-95.
[4] S. Vyazovkin, A.K. Burnham, J.M. Criado, L.A. Pérez-Maqueda, C. Popescu, N. Sbirrazzuoli, ICTAC Kinetics Committee recommendations for performing kinetic computations on thermal analysis data, Thermochimica Acta, 520 (2011) 1-19.
[5] P. Brachi, F. Miccio, M. Miccio, G. Ruoppolo, Pseudo-component thermal decomposition kinetics of tomato peels via isoconversional methods, Fuel Processing Technology, 154 (2016) 243-250.
[6] E.C. Vouvoudi, D.S. Achilias, I.D. Sideridou, Dental light-cured nanocomposites based on a dimethacrylate matrix: Thermal degradation and isoconversional kinetic analysis in N2 atmosphere, Thermochimica Acta, 599 (2015) 63-72.
[7] S. Vyazovkin, Some Basics En Route to Isoconversional Methodology, in: Isoconversional Kinetics of Thermally Stimulated Processes, Springer International Publishing, Cham, 2015, pp. 1-25.
[8] M.J. Starink, The determination of activation energy from linear heating rate experiments: a comparison of the accuracy of isoconversion methods, Thermochimica Acta, 404 (2003) 163-176.
[9] K. Slopiecka, P. Bartocci, F. Fantozzi, Thermogravimetric analysis and kinetic study of poplar wood pyrolysis, Applied Energy, 97 (2012) 491-497.
[10] H.L. Friedman, Kinetics of thermal degradation of char- forming plastics from thermogravimetry. Application to a phenolic plastic, in: Journal of Polymer Science Part C: Polymer Symposia, Wiley Online Library, 1964, pp. 183-195.
[11] M. Zubair, F. Shehzad, M.A. Al-Harthi, Impact of modified graphene and microwave irradiation on thermal stability and degradation mechanism of poly (styrene-co-methyl meth acrylate), Thermochimica Acta, 633 (2016) 48-55.
[12] A.G. Bernardo da Cruz, J.L. Wardell, A.M. Rocco, The decomposition kinetics of [Et4N]2[M(dmit)2] (M = Ni, Pd) in a nitrogen atmosphere using thermogravimetry, Thermochimica Acta, 443 (2006) 217-224.
[13] Ł. Byczyński, M. Dutkiewicz, H. Maciejewski, Thermal degradation kinetics of semi-interpenetrating polymer network based on polyurethane and siloxane, Thermochimica Acta, 560 (2013) 55-62.
[14] K. Chrissafis, K.M. Paraskevopoulos, S.Y. Stavrev, A. Docoslis, A. Vassiliou, D.N. Bikiaris, Characterization and thermal degradation mechanism of isotactic polypropylene/carbon black nanocomposites, Thermochimica Acta, 465 (2007) 6-17.
[15] C.P. Frizzo, M.A. Villetti, A.Z. Tier, I.M. Gindri, L. Buriol, F.A. Rosa, R.M. Claramunt, D. Sanz, M.A.P. Martins, Structural and thermodynamic properties of new pyrazolo[3,4-d]pyridazinones, Thermochimica Acta, 574 (2013) 63-72.
[16] J. Hong, T. Yi, J. Min, C. Cong, K. Zhang, Preparation, thermal decomposition and lifetime of Eu(III)-phenanthroline complex doped xerogel, Thermochimica Acta, 440 (2006) 31-35.
[17] B. Janković, B. Adnađević, S. Mentus, The kinetic analysis of non-isothermal nickel oxide reduction in hydrogen atmosphere using the invariant kinetic parameters method, Thermochimica Acta, 456 (2007) 48-55.
[18] Y. Liu, B. Ma, X. Zhao, Y. Deng, H. Zhang, Z. Wang, The decomposition of Co(NIA)2(H2O)4 in nitrogen atmosphere, Thermochimica Acta, 433 (2005) 170-172.
[19] J. Lv, L. Chen, W. Chen, H. Gao, M. Peng, Kinetic analysis and self-accelerating decomposition temperature (SADT) of dicumyl peroxide, Thermochimica Acta, 571 (2013) 60-63.

[20] K. Pielichowska, Thermooxidative degradation of polyoxymethylene homo- and copolymer nanocomposites with hydroxyapatite: Kinetic and thermoanalytical study, Thermochimica Acta, 600 (2015) 7-19.
[21] P. Ravi, G.M. Gore, A.K. Sikder, S.P. Tewari, Thermal decomposition kinetics of 1-methyl-3,4,5-trinitropyrazole, Thermochimica Acta, 528 (2012) 53-57.
[22] A.A. Vargeese, K. Muralidharan, V.N. Krishnamurthy, Thermal stability of habit modified ammonium nitrate: Insights from isoconversional kinetic analysis, Thermochimica Acta, 524 (2011) 165-169.
[23] M.A. Garrido, R. Font, Pyrolysis and combustion study of flexible polyurethane foam, Journal of Analytical and Applied Pyrolysis, 113 (2015) 202-215.
[24] R. Font, J.A. Conesa, J. Molto, M. Munoz, Kinetics of pyrolysis and combustion of pine needles and cones, Journal of Analytical and Applied Pyrolysis, 85 (2009) 276-286.
[25] J.M. Criado, P.E. Sanchez-Jimenez, L.A. Perez-Maqueda, Critical study of the isoconversional methods of kinetic analysis, J Therm Anal Calorim, 92 (2008) 199-203.

LEGEND OF TABLES

Table 3. Moisture, elemental analysis, ash content and net calorific value of materials studied.

Table 4. Experimental conditions in the thermal decomposition process study of two materials

Table 3. Kinetic parameters obtained for the PU pyrolysis

Table 4. Parameters from the linear equations when applying the Friedman method to

the pyrolysis data of PU, using only the data of the dynamic runs

Table 5. Parameters from the linear equations when applying the Friedman method to the pyrolysis data of PU, using both the data of the dynamic runs and dynamic + isothermal runs

Table 6. Scheme of reactions for combustion of pine needles

Table 7. Kinetic parameters for pine needle combustion

pine needles

Table 8. Parameters from the linear equations when applying the Friedman method to the combustion data of pine needles, using only the data of the dynamic runs with an $N_2$:$O_2$ 4:1 atmosphere

Table 9. Parameters from the linear equations when applying the Friedman method to the combustion data of pine needles, using both dynamic and dynamic + isothermal runs under an $N_2$:$O_2$ 4:1 atmosphere

LEGEND OF FIGURES

Figure 1. Experimental and calculated variations of the degree conversion corresponding to the PU pyrolysis: a) Dynamic run at 10 K/min; b) Dynamic at 10

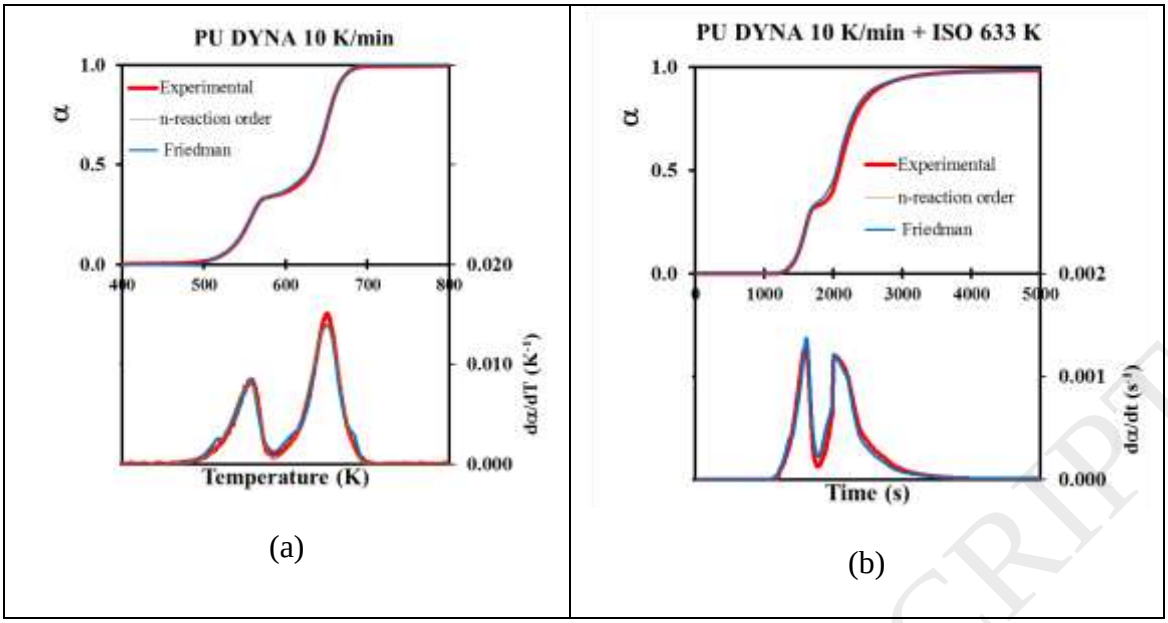


(a) (b)

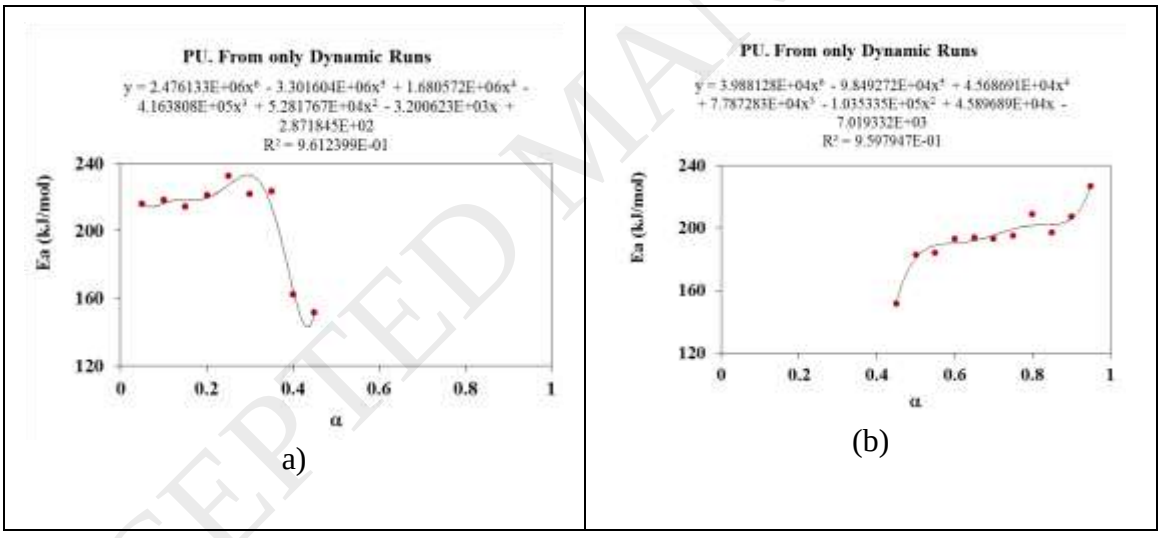


a) (b)

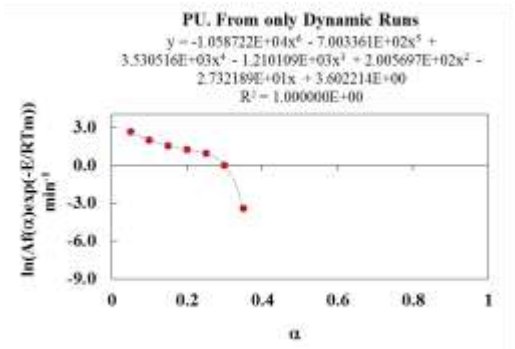


(a)

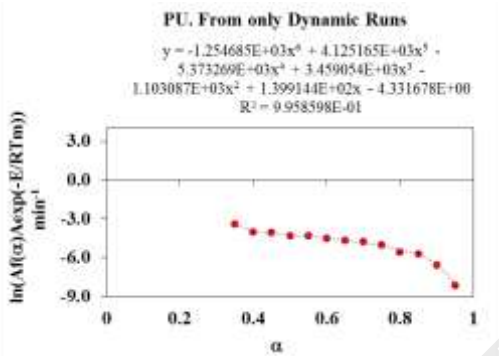


(b)

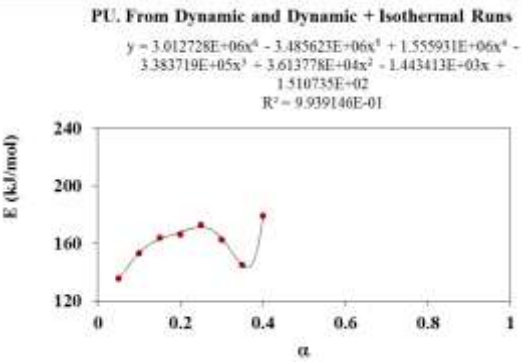


(a)

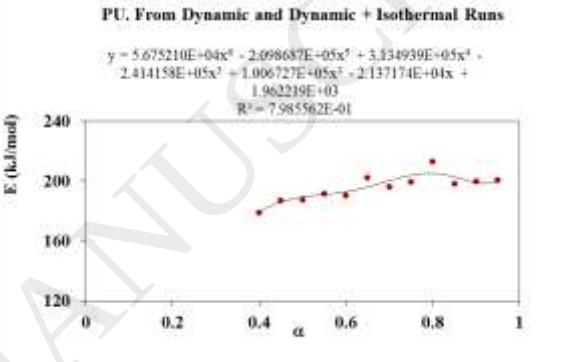


(b)

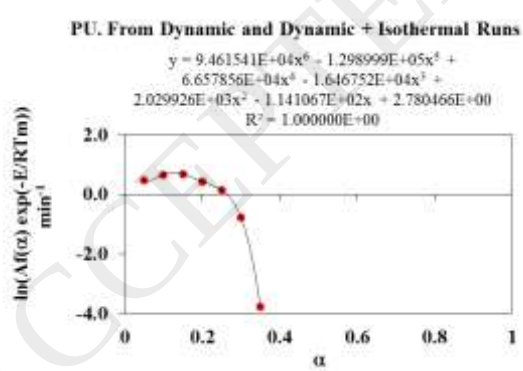


(a)

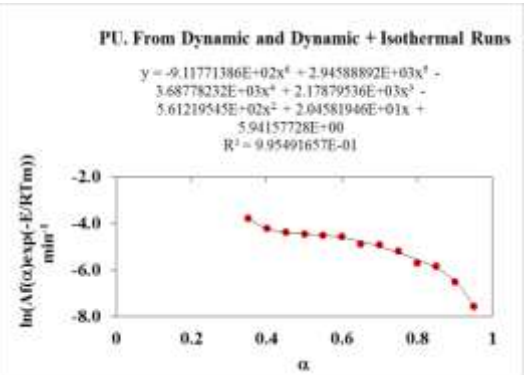


(b)

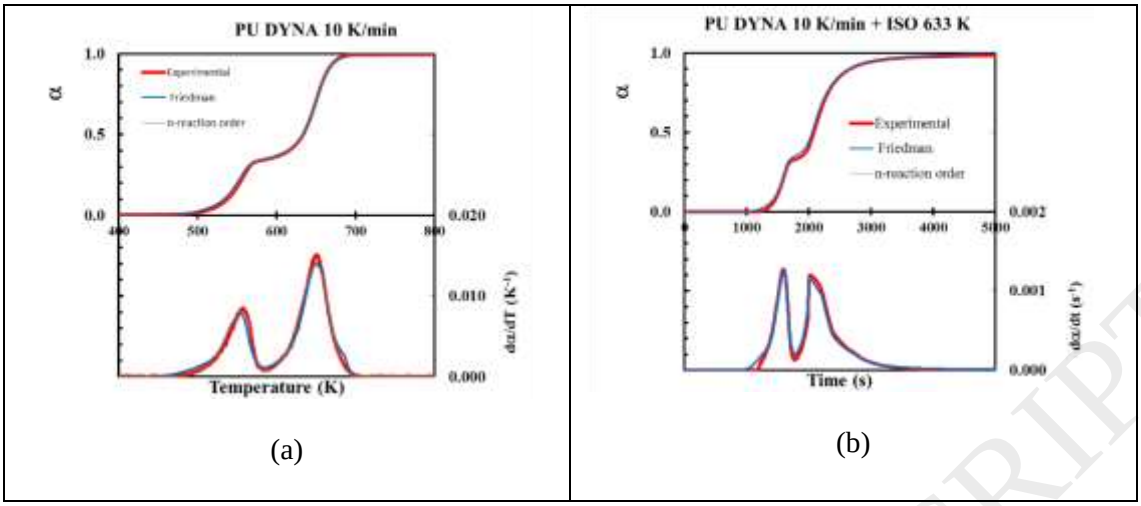


(a) (b)

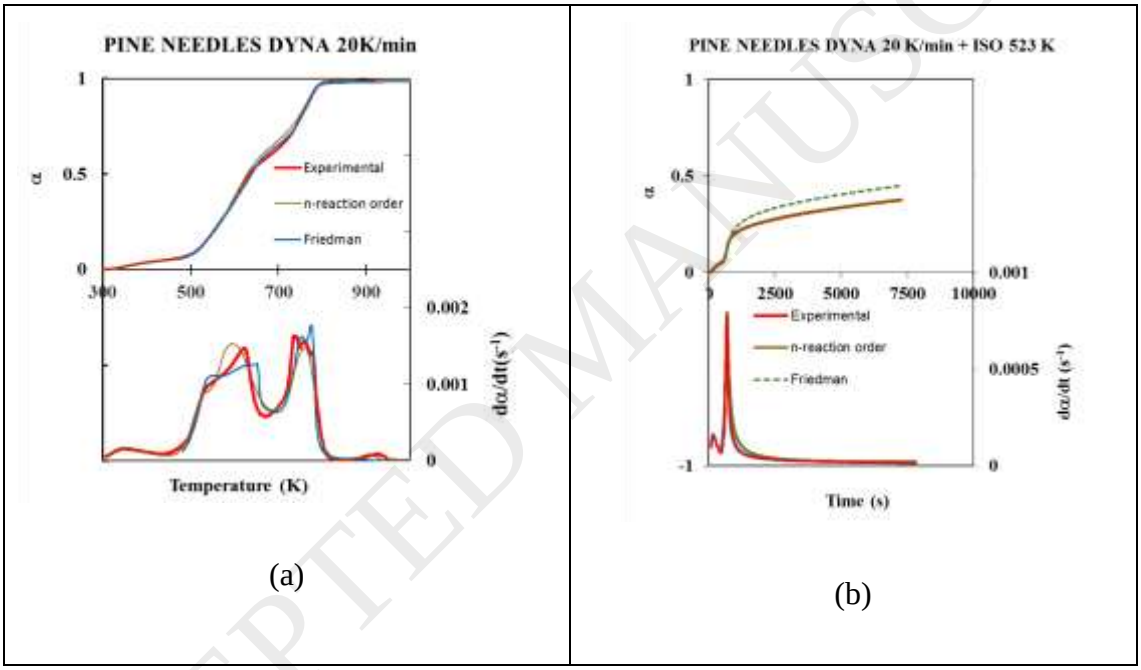


(a) (b)

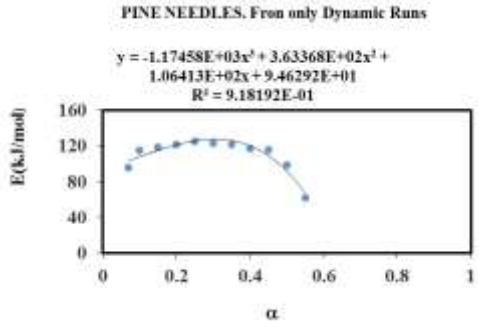


(a)

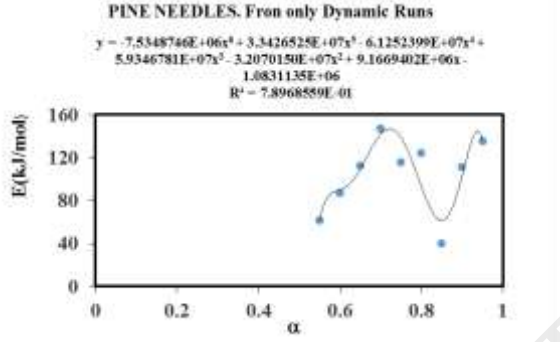


(b)

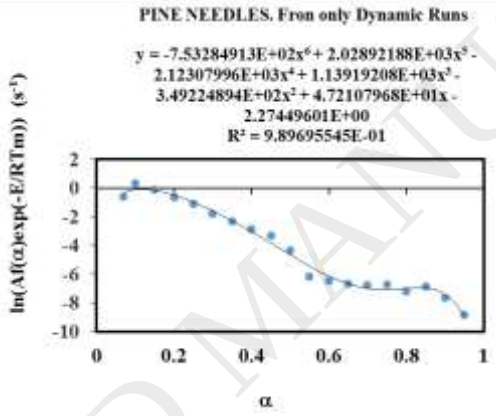


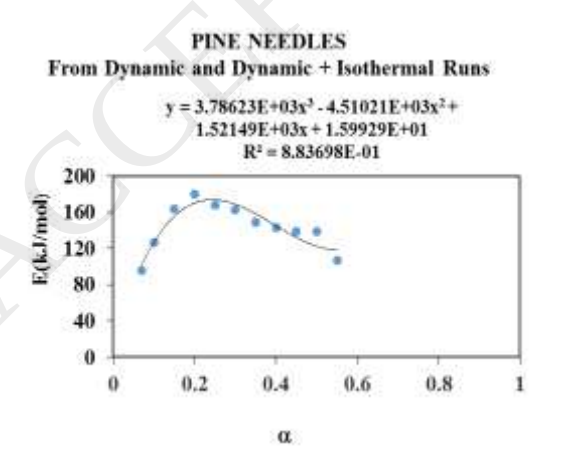


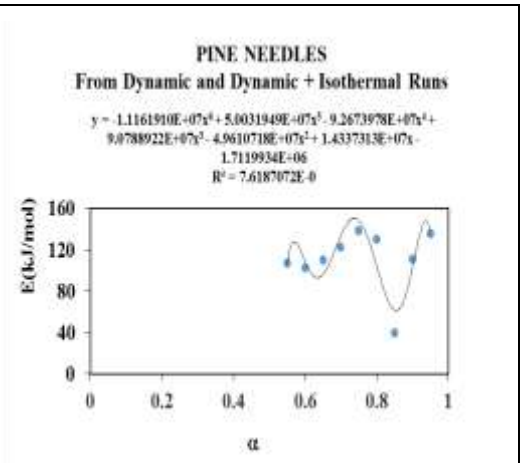

| (a) | (b) |
|---|---|

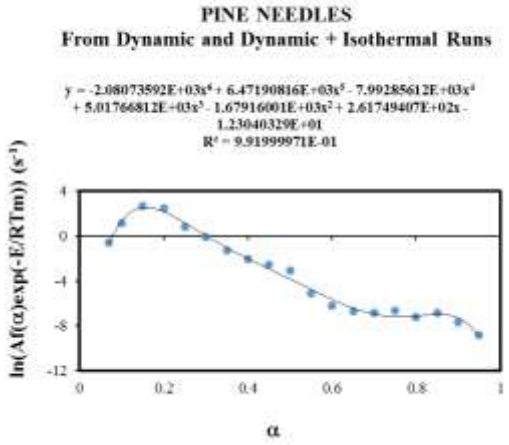


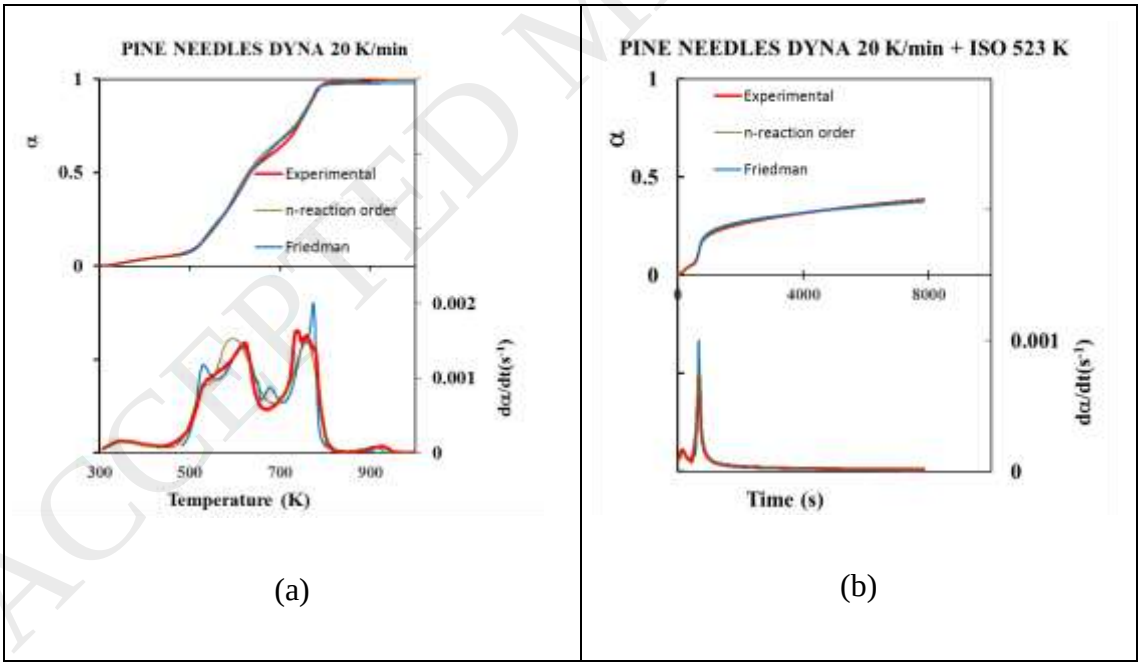


(a) (b)

| | PU | Pine needles |
|---|---|---|
| Moisture (wt. %) | 1.2 | 12 |

| | | |
|---|---|---|
| Analysis on dry basis | | |
| C (wt. %) | 57.79 | 50.4 |
| H (wt. %) | 7.306 | 6.5 |
| N (wt. %) | 5.95 | 0.8 |
| S (wt. %) | <0.01 | 0.01 |
| Ash content (wt. %) | 5.47 | 4.5 |
| O by difference (wt. %) | 23.43 | 37.9 |
| Net calorific value (kJ $kg^{-1}$) | 24,133 | 20,138 |

| | **PU** | **Pine needles** |
|---|---|---|
| Decomposition process | Pyrolysis | Combustion |
| Gas | $N_2$ | $N_2$:$O_2$ 4:1 |
| Mass sample (mg) | 7.5 | 5 |
| Gas flow rate (mL $min^{-1}$) | 100 | 100 |
| Dynamic runs | | |
| Heating rates (K $min^{-1}$) | 5; 10; 20 | 5; 10; 20 |
| Temperature range (K) | 303 - 873 | 298 - 1073 |
| Dynamic + isothermal runs | | |
| Initial heating rates (K $min^{-1}$) | 5; 10; 20 | 5; 10; 20 |
| Isothermal Temperature (K) | 658; 633; 658 | 493; 523;573;623 |

| | Reaction 1 | Reaction 2 |
|---|---|---|
| $V_{i\infty}$ | 0.307 | 0.582 |
| $k_{i0}$ ($s^{-1}$) | $2.044 \cdot 10^{11}$ | $3.247 \cdot 10^{15}$ |
| $E_i$ (kJ $mol^{-1}$) | 142 | 217.5 |
| $n_i$ | 0.81 | 1.25 |

| | Correlation Coefficient | Activation Energy | Tm= 600 K |
|---|---|---|---|
| α | $r^2$ | E(kJ/mol) | ln(Af(α)exp(-E/RTm)) ($min^{-1}$) |
| 0.05 | 0.9862 | 216.29 | 2.60796186 |

| | | | |
|---|---|---|---|
| 0.10 | 0.9699 | 218.48 | 2.00107467 |
| 0.15 | 0.9996 | 214.47 | 1.54617940 |
| 0.20 | 0.9939 | 221.32 | 1.22689138 |
| 0.25 | 0.9993 | 232.94 | 0.92178635 |
| 0.30 | 0.9994 | 222.26 | -0.03873402 |
| 0.35 | 0.7761 | 223.63 | -3.43468296 |
| 0.40 | 0.9502 | 162.49 | -4.02280605 |
| 0.45 | 0.9945 | 151.61 | -4.05173967 |
| 0.50 | 0.9938 | 182.84 | -4.33837802 |
| 0.55 | 0.9957 | 184.20 | -4.34303861 |
| 0.60 | 0.9994 | 193.00 | -4.54039678 |
| 0.65 | 0.9975 | 193.78 | -4.67392399 |
| 0.70 | 1.0000 | 193.15 | -4.79436260 |
| 0.75 | 1.0000 | 195.19 | -5.03236823 |
| 0.80 | 0.9940 | 208.91 | -5.57674404 |
| 0.85 | 0.9980 | 197.03 | -5.74709688 |
| 0.90 | 0.9980 | 207.32 | -6.57743913 |
| 0.95 | 0.9998 | 226.61 | -8.14641533 |

| | Correlation Coefficient | Activation Energy | Tm= 600 K |
|---|---|---|---|
| α | $r^2$ | E(kJ/mol) | ln(Af(α)exp(-E/RTm)) ($min^{-1}$) |
| 0.05 | 0.7648 | 135.68 | 0.4685055 |
| 0.1 | 0.7312 | 153.13 | 0.6550094 |
| 0.15 | 0.8352 | 164.04 | 0.6787759 |
| 0.2 | 0.8863 | 166.06 | 0.4291472 |
| 0.25 | 0.8971 | 173.00 | 0.1358230 |
| 0.3 | 0.8097 | 162.60 | -0.7769031 |
| 0.35 | 0.7449 | 145.15 | -3.7714837 |
| 0.4 | 0.7864 | 179.08 | -4.2148506 |
| 0.45 | 0.9589 | 187.28 | -4.3828927 |
| 0.5 | 0.9481 | 187.58 | -4.4537241 |
| 0.55 | 0.9774 | 191.73 | -4.5087889 |
| 0.6 | 0.9617 | 190.38 | -4.5753621 |
| 0.65 | 0.9784 | 202.30 | -4.8846748 |
| 0.7 | 0.9760 | 196.07 | -4.9201548 |
| 0.75 | 0.9831 | 199.40 | -5.1762788 |
| 0.8 | 0.9912 | 213.10 | -5.7075644 |
| 0.85 | 0.9917 | 198.18 | -5.8251657 |
| 0.9 | 0.9917 | 199.91 | -6.4966541 |
| 0.95 | 0.9955 | 200.69 | -7.5641992 |

| Scheme of reactions | Kinetic equations |
|---|---|
| *Fract. 1 (mainly moisture)*<br>$w_1$ Waste1 ⇒ $v_1$ Volatiles1 | $\frac{d\alpha_1}{dt} = k_{1o}\exp\left[-\frac{E_1}{RT}\right](1-\alpha_1)^{n_1}$ |
| *Fract. 2 (mainly hemicellulose)*<br>$w_2$ Waste2 (+oxygen) ⇒ $v_2$ Volatiles2<br>(the char of this reaction is accumulated to the char formation of cellulose) | $\frac{d\alpha_2}{dt} = k_{2o}\exp\left[-\frac{E_2}{RT}\right](1-\alpha_2)^{n_2}$ |
| *Competitive reactions fract. 3 (mainly cellulose)*<br>$w_3$ Waste3 (+oxygen) ⇒ $v_3$ Volatiles3 + $r_3$ Char3<br>$w_3$ Waste3 (+oxygen) ⇒ $v_{3cp}$ Volatiles3cp + $r_{3cp}$ Ash3cp | $\frac{d\alpha_3}{dt} = k_{3o}\exp\left[-\frac{E_3}{RT}\right](1-\alpha_3-\alpha_{3cp})^{n_3}$<br>$\frac{d\alpha_{3cp}}{dt} = k_{3cpo}\exp\left[-\frac{E_{3cp}}{RT}\right](1-\alpha_3-\alpha_{3cp})^{n_{3cp}}$ |
| *Competitive reactions fract. 4 (mainly lignin)*<br>$w_4$ Waste4 (+oxygen) ⇒ $v_4$ Volatiles4 + $r_4$ Char4<br>$w_4$ Waste4 (+oxygen) ⇒ $v_{4cp}$ Volatiles4cp + $r_{4cp}$ Ash4cp | $\frac{d\alpha_4}{dt} = k_{4o}\exp\left[-\frac{E_4}{RT}\right](1-\alpha_4-\alpha_{4cp})^{n_4}$<br>$\frac{d\alpha_{4cp}}{dt} = k_{4cpo}\exp\left[-\frac{E_{4cp}}{RT}\right](1-\alpha_4-\alpha_{4cp})^{n_{4cp}}$ |
| *Combustion of char formed through reaction 3*<br>$r_3$ Residue3 or Char3 (+oxygen) ⇒ $v_{3c}$ Volatiles3c + $r_{3c}$ Ash3c | $\frac{d\alpha_{3c}}{dt} = k_{3co}\exp\left[-\frac{E_{3c}}{RT}\right](\alpha_3-\alpha_{3c})^{n_{3c}}$ |
| *Combustion of char formed through reaction 4*<br>$r_4$ Residue4 or Char4 (+oxygen) ⇒ $v_{4c}$ Volatiles4c + $r_{4c}$ Ash4c | $\frac{d\alpha_{4c}}{dt} = k_{4co}\exp\left[-\frac{E_{4c}}{RT}\right](\alpha_4-\alpha_{4c})^{n_{4c}}$ |
| *Fraction 5 (mainly CaCO3, decomposes at high temperature)*<br>$w_5$ Waste5 (+oxygen) ⇒ $v_5$ Volatiles5 + $r_5$ Ash5 | $\frac{d\alpha_5}{dt} = k_{5o}\exp\left[-\frac{E_5}{RT}\right](1-\alpha_5)^{n_5}$ |
| Global reaction | $w=1-V=1-(\alpha_1 V_{1inf}+\alpha_2 V_{2inf}+\alpha_3 V_{3inf}+\alpha_{3cp} V_{3cpinf}+\alpha_4 V_{4inf}+\alpha_{4cp} V_{4cpinf}+$ |

| | |
|---|---|
| | $\alpha_{3c}V_{3cinf}+\alpha_{4c}V_{4cinf}+\alpha_5V_{5inf})$ |

Table 7. Kinetic parameters for pine needle combustion

| Reactions | Values of kinetic parameters | Some considerations |
|---|---|---|
| ***Vaporization and pyrolytic reactions*** | | |
| *Fract. 1* | $V_1 = 0.06$<br>$k_{1o} = 1.985.10^4\ s^{-1}$<br>$E_1 = 43.07$ kJ/mol<br>$n_1 = 4.20$ | - Mainly vaporization of moisture |
| *Fract. 2* | $V_2 = 0.19$<br>$k_{2o} = 5.838.10^{11}\ s^{-1}$<br>$E_2 = 137.18$ kJ/mol<br>$n_1 = 2.89$ | - Pyrolysis of mainly hemicellulose |
| *Fract. 3* | $V_3 = 0.34$<br>$k_{3o} = 1.38.10^{19}\ s^{-1}$<br>$E_3 = 233.32$ kJ/mol<br>$n_3 = 7.73$ | - Pyrolysis of mainly cellulose |
| *Fract. 4* | $V_4 = 0.13$<br>$k_{4o} = 8.99.10^{14}\ s^{-1}$<br>$E_4 = 197.31$ kJ/mol<br>$n_4 = 3.58$ | - Pyrolysis of mainly lignin |
| ***Competitive oxidative pyrolysis of fractions 3 and 4*** | | |
| *Fract. 3* | $V_{3cp} = 0.41$<br>$k_{3cp} = 1.065.10^3\ s^{-1}$<br>$E_{3cp} = 80.69$ kJ/mol<br>$n_{3cp} = 0.66$ | -Oxidative pyrolysis of mainly cellulose with ash formation |
| *Fract. 4* | $V_{4cp} = 0.32$<br>$k_{4cpo} = 1.516.10^5\ s^{-1}$<br>$E_{4cp} = 97.49$ kJ/mol<br>$n_{4cp} = 1.66$ | - Oxidative pyrolysis of mainly lignin with ash formation |
| ***Char combustion*** | | |
| *Combustion of Char3 and Char4* | $V_{3c} = 0.07$<br>$V_{4c} = 0.19$<br>$k_{3c} = k_{4c} = 3.323.10^9\ s^{-1}$<br>$E_{3c} = E_{4c} = 166.17$ kJ/mol<br>$n_{3c} = n_{4c} = 0.91$ | -Combustion of char with ash formation |
| ***Other reaction*** | | |
| *Fract. 5* | $V_5 = 0.01$<br>$k_{5o} = 1.596\ 10^{22}\ s^{-1}$<br>$E_4 = 415.7$ kJ/mol<br>$n_4 = 1.00$ | -Decomposition of mainly $CaCO_3$ |

| | Correlation coefficient | Activation Energy | Tm= 725 K |
|---|---|---|---|
| α | $r^2$ | E(kJ/mol) | ln(Af(α)exp(-E/RTm)) ($s^{-1}$) |
| 0.07 | 0.9862 | 96.18 | -0.60852573 |
| 0.1 | 0.9903 | 114.82 | 0.32082873 |
| 0.15 | 0.9668 | 118.41 | -0.10171997 |
| 0.2 | 0.9724 | 121.81 | -0.62408673 |
| 0.25 | 0.9932 | 125.66 | -1.09677153 |
| 0.3 | 0.9983 | 123.04 | -1.77430111 |
| 0.35 | 0.9949 | 121.68 | -2.32070637 |
| 0.4 | 0.9798 | 117.29 | -2.88581389 |
| 0.45 | 0.9657 | 115.63 | -3.29074349 |
| 0.5 | 0.9053 | 98.61 | -4.33020245 |
| 0.55 | 0.7799 | 61.79 | -6.16013226 |
| 0.6 | 0.9370 | 87.16 | -6.43891572 |
| 0.65 | 0.9488 | 112.81 | -6.65130287 |
| 0.7 | 0.9412 | 147.38 | -6.73550751 |
| 0.75 | 0.3922 | 116.18 | -6.69703747 |
| 0.8 | 0.9839 | 124.18 | -7.22453753 |
| 0.85 | 0.2603 | 39.94 | -6.86006205 |
| 0.9 | 0.8269 | 111.00 | -7.66475854 |
| 0.95 | 0.9701 | 135.33 | -8.82079678 |

| | Correlation coefficient | Activation Energy | Tm= 725 K |
|---|---|---|---|
| α | r2 | kJ/mol | ln(Af(α)exp(-E/RTm)) (s-1) |
| 0.07 | 0.9862 | 96.18 | -0.6085257 |
| 0.1 | 0.9563 | 126.78 | 1.13934693 |
| 0.15 | 0.9431 | 163.69 | 2.69976243 |
| 0.2 | 0.9667 | 179.74 | 2.5130807 |
| 0.25 | 0.9702 | 167.95 | 0.84607109 |
| 0.3 | 0.9908 | 162.71 | -0.0520172 |
| 0.35 | 0.9894 | 149.42 | -1.2943281 |
| 0.4 | 0.9442 | 142.78 | -2.0244968 |
| 0.45 | 0.9730 | 138.58 | -2.5747257 |
| 0.5 | 0.9488 | 138.55 | -3.0965862 |
| 0.55 | 0.9283 | 107.08 | -5.091325 |
| 0.6 | 0.9868 | 102.71 | -6.1819177 |
| 0.65 | 0.9937 | 110.37 | -6.6743362 |
| 0.7 | 0.9774 | 122.99 | -6.856799 |
| 0.75 | 0.8903 | 139.03 | -6.6533251 |
| 0.8 | 0.9983 | 130.56 | -7.2287991 |
| 0.85 | 0.2603 | 39.94 | -6.8600621 |
| 0.9 | 0.8269 | 111.00 | -7.6647585 |
| 0.95 | 0.9701 | 135.33 | -8.8207968 |